

# Site Characterization for Tidal Power

Sam Gooch<sup>1</sup>  
Jim Thomson<sup>1</sup>  
Brian Polagye<sup>1</sup>  
Dallas Meggitt<sup>2</sup>

<sup>1</sup>Northwest National Marine Renewable Energy Center, University of Washington Seattle, WA.

<sup>2</sup>Sound & Sea Technology, Lynnwood, WA.

**Abstract** - Tidal In-Stream Energy Conversion (TISEC) is a promising source of clean, renewable and predictable energy. One of the preliminary steps in developing the technology is establishing a standardized and repeatable methodology for the characterization of potential deployment sites. Stationary Acoustic Doppler Profiler (ADCP) velocity data collected at four sites near Marrowstone Island, Puget Sound are used to test the applicability of metrics characterizing maximum and mean velocity, eddy intensity, rate of turbulent kinetic energy dissipation, vertical shear, directionality, ebb and flood asymmetry, vertical profile and other aspects of the flow regime deemed relevant to TISEC. Based on these analyses, the flow at three sites clustered along the east bank of Marrowstone Island (referred to as the “D” sites) are found to be mainly bidirectional and have similar ebb and flood velocities and relatively low levels of turbulent activity. The site near the north point of Marrowstone Island (the “C” site) has higher maximum and mean ebb velocities, but is more asymmetrical and has higher levels of turbulent activity. In addition, methods are applied to data from another Puget Sound site (Admiralty Inlet), and results are compared. A two-dimensional “velocity map” is developed for the more promising “D” sites, showing the spatial variation of velocities throughout the area. This map is based on data collected using a vessel-mounted ADCP in linear transects running roughly perpendicular to the flow at the site. Interpolation between these transects along isobaths yields a rough grid of velocities, from which the velocity map can be determined using a two-dimensional interpolation scheme. Results are promising, although this method may not work well at sites with different bathymetric and geographic characteristics. The methods and conclusions are device-neutral, however device specific considerations will be important prior to developing TISEC sites.

## I. OVERVIEW

Site characterization is one of the first steps in the development of a Tidal In-Stream Energy Conversion (TISEC) project of any scale. As such, it is also one of the first areas of research undertaken by the University of Washington branch of the Northwest National Marine Renewable Energy Center (NNMREC), a newly formed interdisciplinary group focusing on the advancement of TISEC technology.

This research is based on data from two separate projects, both in Puget Sound. One is a Navy-funded project off the coast of Marrowstone Island, intended to demonstrate the

feasibility of TISEC for providing the 25% renewable energy mandated for all defense agencies by the year 2025 [1]. Data from this project are provided by Sound and Sea Technology, a partner of NNMREC. The second is a pilot project in Admiralty Inlet, Puget Sound, undertaken by the Snohomish County Public Utility District (SnoPUD), which has potential to become a utility-scale installation. This would help to fulfill the utility’s obligation under state initiative I-937 to obtain 15% of its electricity from renewable sources by 2020 [2]. NNMREC has partnered with SnoPUD on the project and is currently collecting velocity and environmental data at the site.

This research is divided into three sections. The first is a literature review covering the current state of TISEC site characterization methodologies and techniques. The second is a collection of metrics specifically tailored to TISEC, based on ADCP velocity data collected at a fixed point over a long (1-3 month) period of time. The third section outlines a methodology for determining the small-scale variability in a site’s velocity (in the form of a ‘velocity map’) using data collected from a vessel-mounted ADCP.

## II. LITERATURE REVIEW

### A. Introduction

To date, little literature has been published on methods for field data collection specifically tailored to Tidal In-Stream Energy Conversion (TISEC) site evaluation. Several paper studies have been conducted based on existing tidal current data sources such as the Admiralty Charts in the United Kingdom or the Tidal Current tables published by the National Atmospheric and Oceanic Administration (NOAA) in the United States, [3], [4]. Errors in these predictions can be high, as the predictions are based on vintage surveys and were not originally intended for resource assessment [4]. A study conducted by Black and Veatch found discrepancies of as much as 2 m/s at a site using different tidal atlases [3]. For this reason, field velocity data collection for TISEC site analysis is widely accepted as a necessity, and is a component of all but the first stage of the European Marine Energy Centre’s (EMEC) site selection methodology, the only standard procedure proposed on this topic to date [5].

Direct funding for this research provided by Sound and Sea Technology and the Washington Research Foundation. This material is based upon work supported by the Department of Energy under Award Number DE-FG36-08GO18179. This report was prepared as an account of work sponsored by an agency of the United States Government. Neither the United States Government nor any agency thereof, nor any of their employees, makes any warranty, expressed or implied, or assumes any legal liability or responsibility for the accuracy, completeness, or usefulness of any information, apparatus, product, or process disclosed, or represents that its use would not infringe privately owned rights. Reference herein to any specific commercial product, process, or service by trade name, trademark, manufacturer, or otherwise does not necessarily constitute or imply its endorsement, recommendation, or favoring by the United States Government or any agency thereof. Their views and opinions of the authors expressed herein do not necessarily state or reflect those of the United States Government or any agency thereof.

TABLE I

	Site	Marrowstone Island				Admiralty Inlet			Deception Pass	Tacoma Narrows	
		D9	D10	D11	C5	AI3	AI1	AI2	DP1	TN2	TN3
	Velocity										
	Mean speed (m/s)	0.72	0.73	0.75	0.95	1.26	1.05	1.08	1.95	0.81	1.10
	Max sustained speed (m/s) <sup>a</sup>	2.14	2.12	2.19	2.24	3.25	2.73	2.93	3.95	2.66	2.89
	Eddy intensity (%) <sup>b</sup>	2.9%	3.1%	2.8%	5.2%	5.4%	-	-	-	-	-
	Ebb/flood asymmetry	0.97	0.98	0.93	1.47	1.06	0.97	0.95	1.12	0.58	0.98
	Vertical shear (m/s per m)	0.023	0.024	0.027	0.033	0.031	0.010	0.023	0.015	0.009	0.023
	TKE dissipation (W/m <sup>2</sup> )10 <sup>-5</sup>	1.9	2.2	2.6	7.5	10.8	-	-	-	-	-
	Power										
	Mean power density (kW/m2)	0.42	0.43	0.48	0.98	2.1	1.28	1.51	5.96	0.86	1.44
	Ebb/flood asymmetry	0.9	0.9	0.8	3.9	1.2	0.9	0.9	1.4	0.1	0.9
	Direction										
	Principle axis <sup>c</sup> (deg)	-32	-34	-30	-43	-49	-41	-48	89	-28	-1
	Standard deviation (deg)	10	9	7	14	12	11	6	9	8	6
	Ebb/flood asymmetry (deg)	6	12	9	58	23	15	4	2	4	10
	Vertical Profile										
	Assumed hub height (m)	12.5	11.5	10.7	12.7	27.8	41.9	34.0	19.0	35.0	27.0
	Mean depth (m)	25	23	21	25	56	85	67	39	69	55
	Power law exponent 1/( $\alpha$ ) <sup>d</sup>	5.2	5.1	4.7	3.9	10.1	5.0	4.7	5.8	10.2	4.4
	Standard deviation of $\alpha$	2.5	2.3	3.3	2.7	5.7	3.1	2.2	2.7	4.6	1.6
	% of profiles fit	81%	91%	94%	96%	72%	77%	81%	76%	61%	84%
	Site										
	Measurement duration (days)	33	33	33	33	75	32	32	32	31	31
	Vertical resolution (m)	1	1	1	1	1	2	1	2	1	1
Sampling interval (min)	1	1	1	1	0.5	15	15	15	15	15	
Data collected by	OARS	OARS	OARS	OARS	NNMREC	EH	EH	EH	EH	EH	
Ebb Statistics	Velocity										
	Mean speed (m/s)	0.95	0.95	0.97	1.41	1.5	1.28	1.35	2.20	0.74	1.32
	Max sustained speed (m/s)	2.19	2.24	2.29	3.03	3.41	-2.62	-2.77	-3.95	-1.29	-2.50
	Eddy intensity (%)	2.9%	3.1%	2.9%	5.1%	6.2%	-	-	-	-	-
	Vertical shear (m/s per m)	0.025	0.026	0.028	0.028	0.033	0.009	0.023	0.019	0.011	0.022
	Direction										
	Principle axis (deg)	-30	-28	-26	-23	-60	-49	-51	-88	-31	5
	Standard deviation (deg)	12	10	8	17	11	10	7	8	9	6
	Vertical Profile										
	Power law exponent 1/( $\alpha$ )	4.5	4.5	4.4	5.5	11.3	5.0	4.0	5.2	3.9	4.3
	Standard deviation of $\alpha$	2.5	2.2	2.8	3.8	6.5	3.6	2.2	2.3	2.1	1.4
	% of profiles fit	94%	98%	96%	94%	77%	89%	95%	90%	48%	90%
	Power										
Mean power density (kW/m <sup>2</sup> )	0.61	0.63	0.68	2.2	2.78	1.62	1.98	7.38	0.24	1.70	
Flood Statistics	Velocity										
	Mean speed (m/s)	0.98	0.98	1.04	0.96	1.41	1.31	1.42	1.97	1.28	1.34
	Max sustained speed (m/s)	2.01	1.95	2.04	1.63	3.08	2.73	2.93	3.47	2.66	2.89
	Eddy intensity (%)	2.8%	3.2%	2.7%	5.4%	4.5%	-	-	-	-	-
	Vertical shear (m/s per m)	0.020	0.022	0.026	0.037	0.03	0.011	0.023	0.011	0.008	0.024
	Direction										
	Principle axis (deg)	144	139	144	99	143	146	133	91	153	175
	Standard deviation (deg)	7	7	7	12	12	11	6	9	7	5
	Vertical Profile										
	Power law exponent 1/( $\alpha$ )	6.2	5.9	5.2	2.7	8.9	5.0	5.9	7.2	11.5	4.4
	Standard deviation of $\alpha$	2.7	2.4	4	1.8	4.9	2.3	2.2	3.6	5.1	1.9
	% of profiles fit	82%	81%	90%	97%	65%	61%	58%	45%	63%	76%
	Power										
Mean power density (kW/m <sup>2</sup> )	0.69	0.69	0.81	0.57	2.31	1.77	2.18	5.43	1.77	1.97	

<sup>a</sup> Marrowstone and Admiralty site AI3 maximum "sustained" duration is 5 minutes. For all other sites, duration is 15 minutes due to longer sampling interval.

<sup>b</sup> Eddy intensity and rate of TKE dissipation not available at sites with longer sampling interval.

<sup>c</sup> Angles reported from magnetic north. 180 degrees are subtracted from ebb direction so that an average of ebb and flood directions can be computed.

<sup>d</sup> Assuming vertical profile is of the form  $u(z) = u_0(z/z_0)^{1/\alpha}$ .

### B. Importance of Site Characterization

Velocity data is critical in evaluating a site for TISEC devices, as current speeds are the primary factor in determining the quality of a potential site [6]. Power density is described as:

$$P = 1/2\rho v^3 \quad (1)$$

where  $P$  is power density ( $\text{kW}/\text{m}^2$ ),  $\rho$  is the density of seawater (nominally  $1025\text{kg}/\text{m}^3$ ), and  $v$  is velocity. Because power density scales with the cube of velocity, even modest increases in speed can lead to significant gains in power production [7].

Velocity time series data allow for the calculation of additional metrics (e.g., velocity distribution and tidal ellipses), yielding a more in-depth understanding of the tidal dynamics at a site. Velocity data are used for calculating the maximum forces and stresses that a device may need to withstand, useful for design considerations [5]. These topics are covered in depth later in this review. Field velocity data is also the only basis for performing turbulence calculations, which is critical for the design and siting of TISEC devices and foundations [8]. Additionally, field data are used in the calibration of computational fluid dynamic (CFD) models [5], [9].

### C. Metrics Proposed By EMEC

This section describes the metrics proposed by the EMEC guidelines for tidal resource assessment [5], as well as additional background information where available. The most intuitive metrics, such as velocity distribution, maximum velocities, tidal range, boundary layer approximations and power density are not described here, but are covered in Section III.

### D. EMEC Metrics: Harmonic Analysis

EMEC guidelines state that for later stages of site characterization at least 20 tidal constituents should be resolved, and it should be possible to extract a minimum of 23 tidal constituents using one month of velocity data [5]. It should be noted that while it may technically be possible to extract this many constituents, only a few may have a signal to noise (SNR) ratio high enough to justify their inclusion in a long term prediction. Including additional constituents will likely lead to characterization of noise in the tidal signal, and will actually decrease the quality of the prediction [10]. Additionally, some regionally important constituents may be convolved with others (e.g.  $K_1$  and  $P_1$  in Puget Sound, Washington) because their periods are extremely similar, and will require longer timeseries to determine. A study by Lueck and Lu found that 91% of the flow velocity at a test site in the Cordova Channel, British Columbia could be explained using only the  $M_2$ ,  $S_2$ ,  $K_1$  and  $O_1$  constituents [11]. Much of the tidal signal not explained by these few predominant constituents is generally due to non-tidal variations caused by weather, turbulence, local bathymetric influence or baroclinic circulation and cannot be predicted using harmonic analysis [10].

### E. EMEC Metrics: Tidal Ellipse

The tidal ellipse is defined as the path the currents trace out during one period for a given tidal constituent. For TISEC considerations, a tidal ellipse with a large major and small minor axis is ideal, as this represents a strongly bi-directional flow. This becomes important for devices that may not be able to extract energy from all directions, such as those with no or limited ability to yaw into the direction of the currents. A device with no yaw control would be aligned parallel to the major axis. EMEC guidelines recommend that if the flow direction is off of the major axis by more than 10% for over 5% of the time, a directionality offset in the available resource is to be applied if applicable to the functionality of a specific TISEC device. This metric may not be relevant if a device is able to extract energy from any direction, but should still be considered for the purpose of support structure and yaw tracking.

### F. EMEC Metrics: Turbulence

EMEC has reserved a section for studies of turbulence in its guidelines, but has not established its own specifications to date, instead recommending that recent papers on the topic be consulted [5].

A more recent study conducted at the EMEC test berth focused on defining turbulence at the site. The ADCP was configured with 1m bins in the vertical and 1 second sampling. The study focused on turbulence due to the bottom boundary layer and its vertical penetration. "Turbulent" conditions were defined as any sample having a 1m/s difference between maximum and minimum velocities within a centered 10 minute sample [8]. Two other methods for quantifying turbulence are discussed in Section III, on focusing on large scale structures (termed "eddy intensity") and the other on the rate of turbulent kinetic energy (TKE) dissipation at the Kolmogorov microscale. Other methods for estimating TKE dissipation rates, using variance and spectral techniques, can also be applied to ADCP data [12], [13].

### G. EMEC Metrics: Modeling and Data Comparisons

One of the primary uses of field ADCP data in the EMEC guidelines is model validation and calibration. No particular model is suggested, although a list of possible hydrodynamic models is included. It is specified that the model shall be either 2D or 3D, and information including boundary conditions, frictional parameters and forcing conditions shall be included with proper justification. Once the model has reached equilibrium (this can take 3-5 model days depending on the domain size), the model is to be run for the same length of time as the stationary field survey (nominally 30 days), and results are to be calibrated to the field data [5].

The numerical resolution required to resolve key features of the flow may be on the order of tens of meters in the horizontal direction and only a few meters in the vertical. For 3D models, this may lead to unacceptably high computational expense. Because of this, numerical models are an important component of site assessment, but do not preclude the need for measurements [14].

### H. Additional Metrics

A paper by Lu and Lueck [11] describes several other metrics used to characterize ADCP data. These metrics serve to characterize a site beyond the recommendations of the EMEC guidelines and are potentially useful for TISEC site analysis. These metrics include information about vertical shear, transverse flows, and directional variation as a function of height and time.

## III. STATIONARY DATA ANALYSIS

### A. Introduction and Device Neutrality

This chapter presents a methodology to characterize potential sites for tidal power development by analyzing Acoustic Doppler Current Profiler (ADCP) data collected at fixed locations. Thus far, site evaluation methods have been developed by private industry and are considered proprietary. Because these methods are not subject to public or peer review, it is difficult to determine whether they are accurate, relevant or repeatable at future sites. Here, a standardized suite of publicly available measurement and analysis methods is developed, which can be used to characterize sites so that they may be directly and fairly compared against one another. These methods utilize repeatable metrics that allow for future sites to be judged not only on the quantitative results of the metrics themselves, but by a relative comparison with similar sites. The methodology developed herein is applied as a test case to several test sites. Four of these sites are under consideration for a Navy demonstration project off the coast of Marrowstone Island, Puget Sound [15]. A fifth site under development by the Snohomish County Public Utility District (SnoPUD) lies near Admiralty Head, Puget Sound.

When required, a hub height of half the water column depth is assumed. For the four (D9, D10, D11, C5) sites of the Marrowstone Island case study, this is approximately 13 meters, and is calculated using the free surface height as recorded by the ADCP pressure sensor. Assumed hub height at the Admiralty Inlet site is 27.8 meters. Actual hub-height values are tabulated in Table I. Most metrics are separated into values for ebb, slack, and flood, with all speeds below 0.5m/s considered to be slack. Ebb and flood regimes are determined using a principal axis decomposition as described in Section III. The threshold can be considered an effective “cut-in” speed, but, again, is intended to be device neutral and is well below the actual “cut-in” of all known devices [16]. More importantly, the separation of ebb-slack-flood regimes ensures that the metrics presented are not biased by measurements of no practical importance, such as the fluctuations in velocity direction surrounding slack water. “Summary” statistics reported in Table I are an average of the corresponding flood and ebb statistics, weighted by the number of samples in the ebb and flood regimes.

Analysis presumes that the method of power generation would be in-stream (i.e., hydrokinetic), but nothing further is assumed regarding device specifics or performance. In practice, device specifics will be essential in site development decision-making. However, a device neutral methodology is

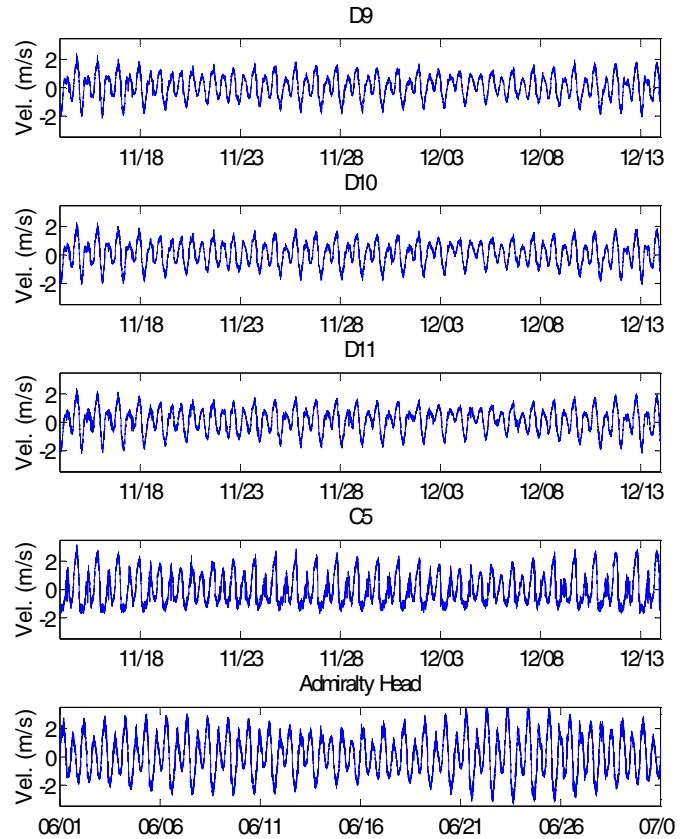


Figure 1. One month timeseries of the five test sites. Ebb is shown as positive velocity and flood as negative.

necessary for world-wide site characterization, and that is the focus herein.

Finally, the analysis presented is sensitive to the sampling scheme used. For consistent results, at least 28 days of stationary ADCP data at 1 min intervals and 1 m resolution are required. Most ADCP manufacturers provide deployment software to assist in configuration and specification of memory and power requirements to meet the recommended sampling.

All analysis is performed in the MATLAB programming environment.

### B. Data Overview

Figure 1 shows a one-month timeseries of each site at the assumed hub height, in which a two neap tides surrounded by three partial spring tides can be observed for the four Marrowstone sites. The Admiralty site begins and ends on a neap and contains two springs. Also of interest is the strong bias towards ebb tides at the C5 site, which is largely due to flow acceleration around the headland at Marrowstone point [17].

### C. Velocity Metrics: Mean Velocity

The simplest possible metric, this can describe whether a site is of any preliminary interest for TISEC (tidal in-stream energy conversion). Velocity magnitudes for every ensemble at hub height are averaged during periods of ebb and flood and using all ensembles, including those at slack. Note that the velocity magnitude refers only to the horizontal components,

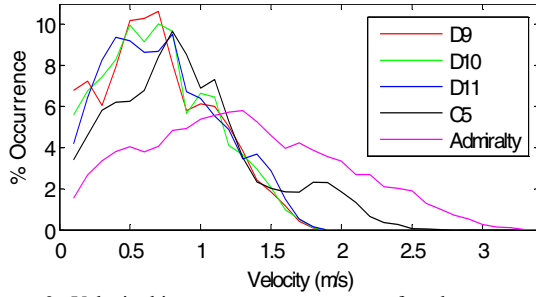


Figure 2. Velocity histograms as a percentage of total occurrences.

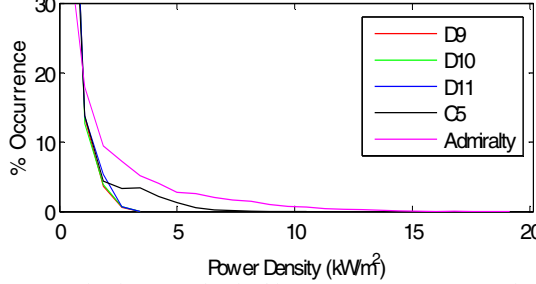


Figure 3. Kinetic power density histograms as a percentage of total occurrences.

and does not include the component in the vertical direction. Results are tabulated in Table I.

#### D. Velocity Metrics: Maximum Sustained Velocity

Maximum sustained velocity is a measure of the highest velocity “sustained” for a period of 5 minutes or more. This is important for preliminary site evaluation as well as turbine design considerations. This is similar to the metric proposed by EMEC, although the maximum velocity must be sustained for 10 minutes to meet their criteria [5].

Ebb and flood hub height velocities are averaged in 5 minute windows. From these, the 5 minute window with the highest mean velocity is found. Note that while higher instantaneous velocities occur elsewhere in the data, it is not “sustained” for any period of time and is of less relevance.

Results are tabulated in Table I.

#### E. Velocity Metrics: Velocity and Power Histograms

Velocity and power histograms provide a simple way to visualize the available resource at a site. The histograms indicate what percentage of the tidal cycle is useful for power generation. This metric is similar to the velocity distribution metric proposed by EMEC.

The MATLAB routine for creating histograms is used. Results for each histogram bin are reported as a percent occurrence. Average power density is computed by finding the power using the hub height velocity from every ensemble using (1), and then taking the average of that number. Note that this is not the same as taking the cube of the average velocity. As in the EMEC recommendations, 0.1 m/s bins are used [5].

As shown in Figure 2 site C5 has a much higher occurrence of larger velocities than the D sites. This is even more apparent in the kinetic power density shown in Figure 3 where the power at C5 is in excess of 5 kW/m<sup>2</sup> at times, whereas the D sites rarely exceed 2.5 kW/m<sup>2</sup>. Admiralty Inlet is again the overall highest. Comparison of the Marrowstone sites

demonstrates the intensification of small differences in velocity upon conversion to power.

#### F. Velocity Metrics: Eddy intensity

Eddy intensity ( $I$ ) is a quantification of the ratio of mesoscale velocity fluctuations to the background velocity. These velocity fluctuations are characterized as turbulent structures on many different length scales caused by bathymetry and flow conditions of the same scale. These structures advected past the point of observation by the mean flow and are thus not expected to be useful for power generation [18].

Eddy intensity is assessed using the following formula [19]:

$$I = \left\langle \frac{v'}{\bar{v}} \right\rangle - \left\langle \frac{n}{\bar{v}} \right\rangle \quad (2)$$

where  $I$  is the eddy intensity (expressed as a ratio),  $v'$  is the velocity anomaly,  $\bar{v}$  is a 15 minute centered difference velocity average, and  $n$  is the intrinsic noise in the ADCP measurement (depends on the working frequency, bin size, and pings per ensemble), which will bias eddy intensity measurements high [20]. The noise is 1.1 cm/s for the Marrowstone sites and 2.9 cm/s for the Admiralty site. Note that the angle brackets represent a mean over the entire data set. All quantities are computed at the bin closest to the assumed hub height. The velocity anomaly  $v' = v - \bar{v}$  represents the velocity with the temporal mean removed, and is calculated every for every observation using the centered difference running average  $\bar{v}$ . The time scale for the running average is chosen as a compromise between including enough individual observations to obtain a meaningful velocity anomaly and having a short enough window that the tide has not changed significantly (i.e., quasi-stationarity). This quantity is then averaged to create a single metric (the eddy intensity,  $I$ ), for the site.

Average eddy intensities are tabulated in Table I. As expected, C5 has an eddy intensity slightly higher than the D sites. This is to be expected, as the Marrowstone headland likely generates eddies which are advected past the C5 site by the ebb currents [17]. Similarly high intensities on the flood tide are likely due to the weak mean velocities in the denominator of the metric, which result in a relatively high eddy intensity ratio. The Admiralty site also has higher eddy intensity on the ebb, likely due to the acceleration around Admiralty Head.

#### G. Velocity Metrics: Rate of Turbulent Kinetic Energy Dissipation

The rate of dissipation of turbulent kinetic energy (TKE) is a measure of how fast energy contained in turbulent motion is actually dissipated as heat and sound at a molecular (micro-scale) level. This is expressed in W/m<sup>3</sup>, and is the rate of energy dissipation per unit volume (i.e., a true loss of energy from the flow, as opposed to advection of energy by the flow). This quantity does not describe the large-scale turbulent features quantified in the aforementioned eddy intensity metric, but only the actual dissipation occurring at a micro-scale. Thus, the resulting values for TKE dissipation rates are

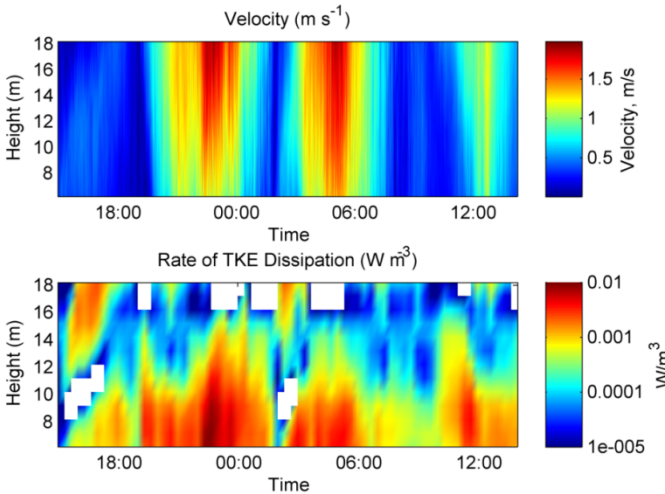


Figure 4. A 24-hour sample of velocity (top panel) and corresponding TKE dissipation rates at site D9.

quite small, and probably of negligible concern for device performance. However, the TKE dissipation rate does provide a useful tool for comparing sites.

The structure function method described by Wiles et al. [21] is used to compute the rate of TKE dissipation. The basic premise lies in using the turbulent component of the velocity data (velocity with the temporal mean removed, as in the section on eddy intensity) to determine the presence and behavior of eddies at each specific point in time and space (in the  $z$  direction, since the ADCPs are stationary and uplooking).

The calculation begins by setting up the 2-dimensional structure function:

$$D(z, r) = \overline{(v'(z) - v'(z + r))^2} \quad (3)$$

where  $D(z, r)$  is the mean-squared velocity fluctuation between two points separated by a distance  $r$ . Velocity fluctuations on the scale of  $r$  are largely due to turbulent structures of the same length and corresponding velocity scales. The value of  $r$  chosen must be smaller than the largest eddies – for the test cases presented here, a conservative value of 5 meters is used. As described in the section on eddy intensity,  $v'$  represents the velocity anomaly, or the velocity with the running average removed. Using the Kolmogorov cascade theory, these characteristic scales are then used to determine the rate of TKE dissipation, expressed as  $\epsilon$ , when fitted to a function of  $r^{2/3}$ :

$$D(z, r) = N + (C_v \epsilon^{2/3}) r^{2/3} \quad (4)$$

where  $N$  is an offset that represents uncertainty due to noise, and  $C_v$  is a constant, which in atmospheric studies is approximately 2.1 [22]. The length-scale parameter  $r$  is from the previous equation. A successful  $r^{2/3}$  fit validates the Kolmogorov cascade assumption. As expected, the velocity difference from a point will grow as the distance from that point becomes larger. Since  $C_v$  is a constant  $\epsilon$  is the only independent variable, and therefore lines with higher slope have greater rates of TKE dissipation.

A sample 24-hour result from site D9 is shown in Figure 4. This is typical of the entire deployment, and sub-set is shown

simply for display purposes. As expected, the rate of TKE is greatest in the boundary layer near the seafloor, and is also generally greatest when the tides are strongest. Some anomalies are present during slack water, but this is to be expected, as a strong ebb/flood tidal shift is likely to cause dissipation. Averaged results for the entire deployment are shown in Table I. C5 has a rate of TKE dissipation an order of magnitude larger than the D sites, which suggests a more turbulent environment, and is consistent with the eddy intensity metric. Again, it is the relative comparison of  $\epsilon$  between sites that is useful for tidal power evaluation, as opposed to the absolute  $\epsilon$  value.

#### H. Velocity Metrics: Vertical Shear

The shear forces exerted by strong (1-3m/s) currents in a dense fluid such as water are significant from a mechanical design standpoint. The turbines must be designed to withstand not only the axial force exerted by the mean component of velocity, but also the shear force created by the velocity variations over the rotor span. These variations are due to the shape of the boundary layer as well as turbulent structures with length scales on the order of the size of the turbine. This makes them especially pertinent, as many turbines will likely be placed within the sea floor boundary layer. This metric is similar to that proposed by Lueck and Lu [11].

The shear is calculated as a centered-difference using the bins below and above the hub height. Ebb and flood regimes are considered separately. The average shear is expressed as a scalar magnitude:

$$\frac{d|v|}{dz} = \frac{|v_{hh-1} - v_{hh+1}|}{\Delta z} \quad (5)$$

where the subscript “ $hh$ ” denotes the bin closest to hub height. Note that while only the velocity magnitude is considered, the flow direction of each velocity component should be roughly similar. If the flow direction changed greatly across the rotor disc but maintained its magnitude, this method would result in underpredictions, as velocities pointed in exactly opposite directions with equal magnitudes would show zero shear. However, cases where flow direction is very different likely occur around slack water when the tidal direction is shifting, and these profiles have already been eliminated using the 0.5m/s threshold.

Average vertical shears are tabulated in Table I. All sites have roughly the same shear on ebb tides, whereas on the flood the D sites are lower and the C5 site is higher. This is likely a function of the shape of the boundary layer. For practical application, these values can be multiplied by the rotor diameter to estimate the change in velocity from the bottom to the top of the rotor sweep. Note that this input condition may be changed by the presence of a turbine, which may homogenize the upstream flow.

#### I. Velocity Metrics: Asymmetry of Ebb/Flood Power and Velocity Magnitude

An asymmetry in the velocity pattern can cause strong power generation on one side of the tidal cycle and weak generation on the other. This has implications for the total



power produced, as well as the usefulness of the power, as producing lots of electricity twice a day (i.e., only on one stage of the tide) is generally not as useful more balanced production four times a day. Recent research has shown TISEC devices may also affect sediment transport where large velocity asymmetries exist [23].

The power and velocity asymmetries are computed as a simple ratio of  $P_{ebb}/P_{flood}$  and  $v_{ebb}/v_{flood}$ , respectively, where  $P$  and  $v$  represent the mean power density and velocity magnitudes.

The D sites are all roughly equal in power availability on ebb and flood tides. The C5 site, in contrast, has 50% more ebb velocity and almost four times the power availability on the ebb tide. Results are tabulated in Table I.

#### J. Directionality Metrics: Principal Axis Decomposition

Characterizing the principal axes of the tides is important for several reasons. It is a rigorous method of determining where ebb and flood regimes begin and end, which can be somewhat difficult to determine because of the two-dimensional nature of tidal currents. Treating ebb and flood regimes separately is important because each regime may have very different characteristics, and if treated together much of this information is lost. Almost all metrics treated in this document are based on the ebb-flood separation, and as shown in Table I, it is often important to present the ebb and flood values for metrics as well as a weighted average.

The principal axis decomposition is used here is based on code described in John Boone’s book *Secrets of the Tide* [10]. This process essentially defines a new coordinate system where the principal axis (the x axis in this case) passes through the mean value and minimizes the sum-squared error of the data set. The principal axes at each site are shown in Table I. Note that the “principal axis” encompasses both ebb and flood tides, and is therefore different than the mean angle values presented for ebb and flood tides in Table I.

#### K. Directionality Metrics: Directional Deviation and Asymmetry

Turbine models designed for bi-directional tides may not have sufficient yaw ability for asymmetrical ebb and flood conditions, and may not be able to efficiently extract energy from these off-axis currents [16]. Asymmetry is a measure of the bi-directionality of the ebb and flood flows. Deviation is a

measure of the amount of directional deviation within the ebb and flood regimes. Large asymmetry or a large deviation in one regime could also lead to strong power generation on one half of the tidal cycle, and very little generation on the other. Furthermore, asymmetrical or deviant currents can indicate complex geometry in the region, which could increase the variability of tides and create a need for more precise and therefore more costly “micrositing” measures [11]. This could also potentially create future complications for placing multiple turbines at a site.

Asymmetry is computed as the difference between ebb and flood angles. The direction is not particularly meaningful, so an absolute value is used:

$$Asymmetry = |\theta_{ebb} - \theta_{flood} - 180| \quad (6)$$

Using this formula, a perfectly bi-directional tide would have an asymmetry of zero degrees. Deviations are calculated as a simple standard deviation of the mean angles within each regime.

As shown in Figure 5, site C5 is highly asymmetrical, and also has the largest standard deviation on both flood and ebb. C5 has the largest velocity magnitudes of any site, although only on the ebb tide. Asymmetries are tabulated in Table I. Note that the angles presented here are different than the principal axes, which encompass both ebb and flood tides.

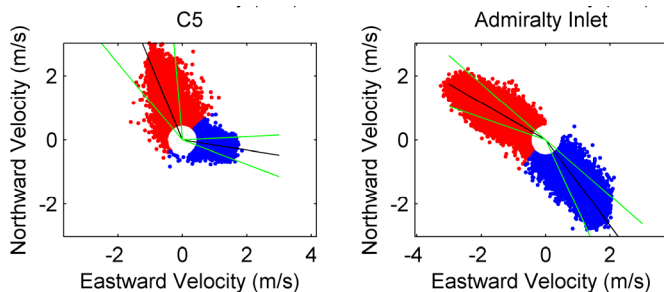
#### L. Vertical Profile Metrics: Power Law Approximation

Tidal currents are generally maximal near the surface and diminished near the seabed. Understanding the reduction in velocity within the bottom boundary layer is essential for designing turbine foundations and determining a desirable hub-height. It has been suggested by previous studies [24] that the boundary-layer behavior of a fluid is best approximated by a power law of the form:

$$V(z) = V_0 \left(\frac{z}{d}\right)^{\frac{1}{\alpha}} \quad (7)$$

where  $V_0$  is the surface velocity,  $d$  is the depth of the fluid,  $V(z)$  and  $z$  are the velocity as a function of depth and depth of the water of fluid, and  $\alpha$  is the empirical constant, nominally 7 or 10 [24], [5]. The ability to model data with such a simple approximation is valuable for making generalizations based on sources of limited data, such as NOAA surface velocity predictions, which can be extrapolated downwards to predict the velocities at the hub heights. Note that the purpose of this analysis is solely to determine the correct power law exponent for use in these predictions, and not to attempt to describe the activity at the site in terms of a single formula.

Instead of fitting a specified exponent such as  $1/7^{\text{th}}$  to the data, this parameter is left as the dependent variable and is optimized through a least-squares fitting using the FIT toolbox in MATLAB. The fitting is performed for 15 minute average velocity profiles with all speeds at hub height in excess of 0.5 m/s. Fits with large residuals ( $R^2 < 0.5$ ) are excluded. Note that most profiles with poor fits occur near the threshold velocity (0.5 m/s) where flow has reversed in part of the water column and are not of practical importance for resource assessment or device performance evaluation. Velocity



	C5	Admiralty Inlet
Ebb	-23±17°	-60±11°
Flood	99±12°	143±12°

Figure 5. Mean axes and standard deviations of ebb (red) and flood (blue) tides at hub height. Angles of mean axes and corresponding standard deviations are given in degrees CW from magnetic north

profiles are characterized for ebb and flood tides, as well as in aggregate.

Power law fits are shown in Table I. At the Marrowstone sites, 80-90% of the data above 0.5m/s is well-described power law (i.e., the power law explains the observation). This number is closer to 70% at the Admiralty site. However, the average power law exponent for all profiles must be viewed with caution. This fit attempts to describe a wide range of data, whose behavior cannot be entirely accurately modeled with any single formula. It is likely that profiles nearer to the peak tide have a different curve than the average profile.

### M. Conclusions

A set of methodology is described to analyze stationary ADCP data for the purpose of tidal power site characterization. Using sites along the northern and eastern shores of Marrowstone Island as case studies, it is shown that average power density is not sufficient to describe the suitability of a site. Although Marrowstone C5 has substantial power density, the in-stream resource is asymmetric (ebb dominated), turbulent, and directionally variable compared with the more laminar sites of D9, D10, and D11. The metrics presented in this section are intended to be used in the TISEC selection process, and are designed to be device neutral. Further analysis will require specific information about the nature of the TISEC device with regard to its height, diameter, yaw capacity, response time and failure modes, among others [16]. It is likely once a device is selected additional parameters not discussed in this report will become relevant for final site selection.

## IV. MOBILE DATA INTERPOLATION

### A. Introduction

It is well known that the power input to a TISEC device scales with the cube of the current velocity, and therefore proper siting is critical to the success of an installation [4]. What is less clear at this point is the effect of “micrositing”, or the analysis of turbine placement on the scale of 10s of meters at a given location. It has been recommended in previous

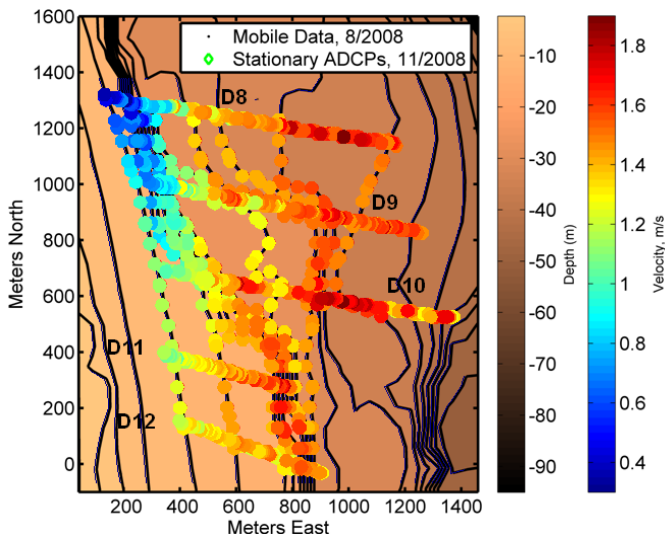


Figure 6. Velocities interpolated along isobaths using mobile ADCP data.

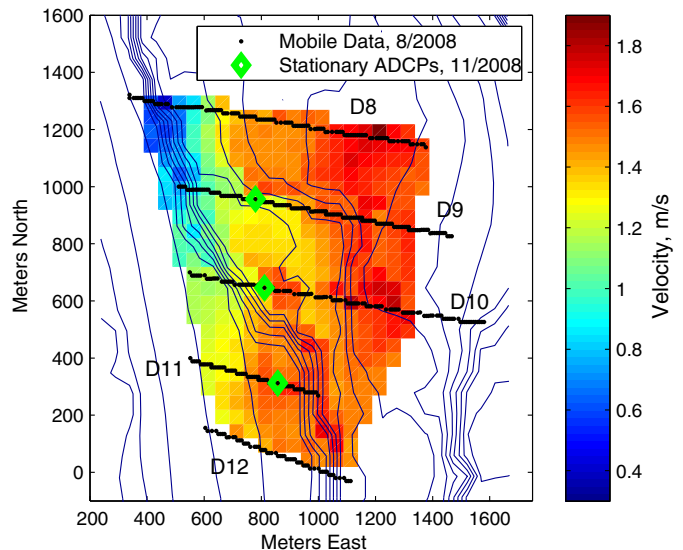


Figure 7. 2D “bathymetry-following” velocity map constructed from data interpolated along isobaths.

studies that 3D modeling and multipoint velocity measurements be undertaken before turbines are deployed, although in many cases TISEC devices are also constrained to a particular water depth and/or hub height, which limits the amount of freedom in their placement [16]. This report intends to address the effect of micrositing for the Marrowstone Island site by using mobile velocity data to determine the spatial variation in the kinetic resource. This data was collected by Evans-Hamilton, Inc. and was originally used to determine the placement of the four stationary ADCPs, whose data were used in the previous section.

The basis of this analysis is an interpolation of mobile data measurements made in linear transects running roughly perpendicular to bathymetry and flow shown in Figure 6. Mobile data measurements are taken from transects made by Evans-Hamilton intended for the selection of the four stationary Marrowstone ADCPs. Data from the three “D” transects are used, as well as the neighboring D8 and D12 transects. Bathymetric data are taken from the NOAA National Geophysical Data Center’s US Coastal Relief Model Grids, which have a resolution of 3 seconds [25]. Bathymetry data within a certain range (nominally 50 meters) of ADCP data is then found, and if multiple points meet the criteria, only the closest one is used. This is repeated for all transect points. Isobaths (lines of constant depth) which intersect multiple transects are flagged, as these form the basis of the interpolation. Velocities are then interpolated along the length of these isobaths between the known values at the transects and using the points from the interpolated bathymetry. This is accomplished by computing the along-isobath distance between transects and performing a spline interpolation across all transects which creates a smooth transition between known values. Using a linear or nearest fitting routine does not take advantage of the ability to interpolate across multiple transects, which allows for more realistic modeling of where points of inflection (velocity maxima and minima) will occur. For this study, data collected during the ebb tide is used, as it is of higher quality than the



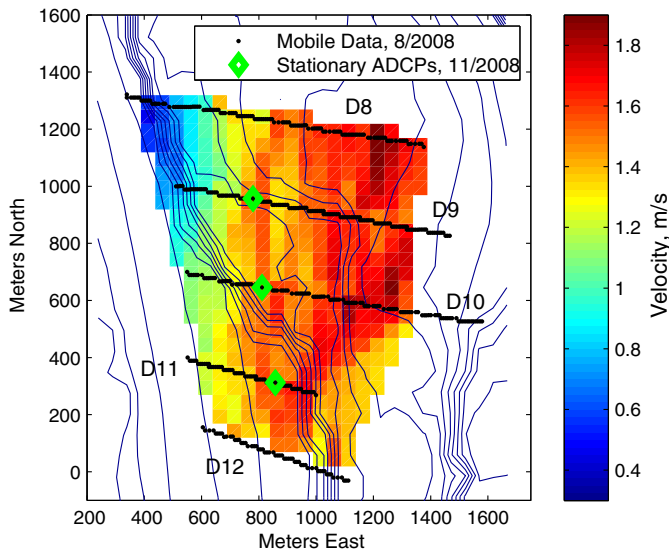


Figure 8. 2D velocity map interpolated using only transect data.

flood data due to technical problems during the collection process [15].

The foremost assumption in making these calculations is that flow will tend to follow the bathymetry at a site. From a fluid mechanics standpoint, this is justified by the conservation of vorticity, which states that the angular momentum of any spinning body (such as an eddy being advected by the tides) is conserved [26]. Since a change in water depth will cause the relative vorticity of such a body to change, these features will tend to follow lines of constant depth so as to maintain their vorticity. This is a crude assumption, but of practical use when a full numerical model is not available.

Another assumption taken in making the interpolations is that the phase difference across transects is negligible. This is necessitated by a lack of co-temporal stationary ADCP data, which could be used to determine the peak ebb and flood and therefore adjust for phase differences as a function of position and time of data acquisitions. However, since the area surveyed in this case is relatively small (less than 1km in

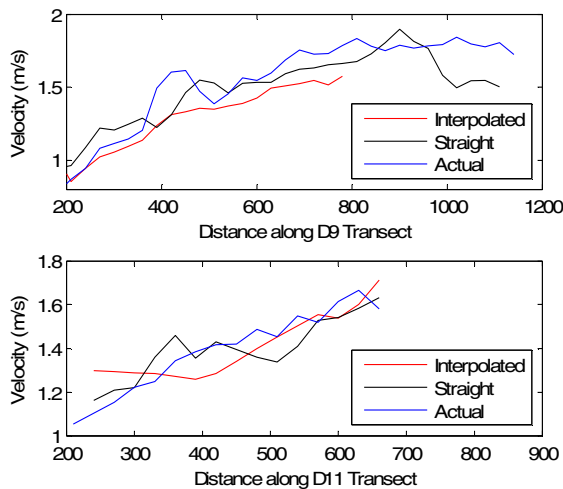


Figure 9. 'Skill' test of the bathymetric and interpolated 2D velocity mapping methodologies.

length) and the surveys were performed quickly (in about 35 minutes), these variations are neglected. A harmonic decomposition of stationary data collected later at the same site shows that the two largest constituents, the  $M_2$  and  $K_1$ , vary between sites by a maximum of only 3.4 and 7.3 minutes, respectively. It is important to keep in mind that all velocities used in this analysis are instantaneous and occur near peak ebb or flood, but are still only snapshots and do not necessarily represent the absolute maximum velocities.

The basic interpolation map is shown in Figure 6 using an arbitrary 1 meter isobath interval. While this yields some useful information about the site, further analysis provides more useful metrics for the purpose of siting TISEC devices.

### B. 2-D Bathymetry-Interpolated Velocity Map

A useful result for site analysis is a 2D "velocity map" of currents at a site, shown in Figure 7. This provides an easier way to visualize trends in currents than looking at raw data. The velocity map is made by performing an additional 2D interpolation of the transect data and the data interpolated along the isobaths using GRIDDATA. Note that in areas where no isobath interpolation exists the map has been cropped, as data interpolated between transects alone has little physical basis. For comparison, a velocity map interpolated using only data collected along transects is shown in Figure 8.

### C. 'Skill' Test

While it is easy to qualitatively compare the results of the bathymetric and interpolated methods, a more rigorous approach for quantifying the quality of the results is of more practical value. A 'skill' test for the two methods consists of removing one of the middle transects (D9 or D11) and making a comparison between the measured velocity and the velocity predicted by interpolation. The results are generally truncated for the interpolated method, as this relies on the isobath-transect intersections which did not occur along the entire length of the middle transects. Results show that in some cases, the basic interpolation method actually performs better than the bathymetric method, indicating that the assumption that flow follows bathymetry may not be accurate to the degree necessary for the bathymetry-following interpolation scheme to produce significant gains over the basic interpolation scheme. However, both methods are still relatively accurate, with error rarely exceeding 0.1 m/s.

Further error in the bathymetry-following method occurs when bathymetry has severe shifts or "doubles back" on itself, which requires corresponding shifts in projected flow. These shifts are most likely not non-physical, and in some cases provide contradictory results to the ADCP data. GRIDDATA averages these results, although a more rigorous approach would use only the ADCP data. Errors in the non-bathymetric interpolated method are caused by an entirely non-physical interpolation process, which in this case uses a primarily north-south route between the primarily east-west transects. This causes the non-physical artifacts such as "streaks" and sudden jumps in velocity.

#### D. Other Considerations

Note that these velocity maps are based on ebb data. Flood data would likely produce a different map, based on local bathymetry and features such as headlands, which can create large scale eddies in one direction [6]. Unfortunately, flood data for this site is more erratic due to technical problems during collection, and preliminary map iterations were of lower quality as those constructed using ebb data.

#### E. Conclusions

Preliminary trials of the velocity resource map have been relatively promising. However, these results may not apply to all sites, as results are highly dependent on local bathymetry and flow conditions. The assumption of flow following bathymetry will not be valid if the mean flow is not roughly perpendicular to isobaths. In sites with more complex bathymetry, flow will most likely not follow the contours of the seafloor closely and the assumption will break down.

Future iterations of this analysis might employ additional interpolation techniques, such as a “progressive vector diagram”, where known velocity directions are extrapolated to neighboring transects, and so on. These extrapolated lines can then form the basis of a spline velocity interpolation similar to that used in the bathymetry-following scheme. This is designed to simulate a Lagrangian “particle following” model from Eulerian (fixed coordinate) data, and is commonplace in atmospheric and oceanic sciences [27]. This would provide a reasonable substitute for bathymetric interpolation in areas where such an assumption is illogical or produces erratic results.

#### REFERENCES

- [1] The Associated Press. (2009, March) Navy to test tidal power in North Puget Sound. [Online]. [http://www.oregonlive.com/environment/index.ssf/2009/03/navy\\_to\\_test\\_tidal\\_power\\_in\\_no.html](http://www.oregonlive.com/environment/index.ssf/2009/03/navy_to_test_tidal_power_in_no.html)
- [2] Sam Reed. (2006) Initiative 937. [Online]. <http://www.secstate.wa.gov/elections/initiatives/text/i937.pdf>
- [3] Black and Veatch, "PHASE II UK Tidal Stream Energy Resource Assessment," Isleworth, 2005.
- [4] George Hagerman and Brian Polagye, "Methodology for Estimating Tidal Current Energy Resources and Power Production by Tidal In-Stream Energy Conversion (TISEC) Devices," in *EPRI North American Tidal In Stream Power Feasibility Demonstration Project.*: EPRI, 2006.
- [5] Claire Legrand, "Assessment of Tidal Energy Resource," The European Marine Energy Center, London, 2009.
- [6] Brian Polagye, Mirko Previsic, and Roger Bedard, "Tidal In-Stream Energy Conversion (TISEC): Survey and Characterization of SnoPUD Project Sites in the Puget Sound," in *EPRI North American Tidal In Stream Power Feasibility Demonstration Project.*: EPRI, 2007.
- [7] Ian Bryden and G T Melville, "Choosing and evaluating sites for tidal current development," vol. 218, 2004.
- [8] E. Droniou and J. V. Norris, "Update on EMEC activities, resource description, and characterisation of wave-induced velocities in a tidal flow," in *7th European Wave and Tidal Energy Conference*, Porto, Portugal, 2007.
- [9] Burton Hamner, "Tacoma Narrows Tidal Power Feasibility Study," Seattle, 2007.
- [10] John D. Boon, *Secrets of the tide: tide and tidal current analysis and applications, storm surges and sea level trends.*: Horwood Publishing, 2004.
- [11] Youyu Lu and Rolf G. Lueck, "Using a Broadband ADCP in a Tidal Channel. Part I: Mean Flow and Shear," *J. Atmospheric and Oceanic Tech.*, vol. 16, pp. 1556-1568, November 1999.
- [12] A. E. Gargett, "Velcro measurement of turbulence kinetic energy dissipation rate epsilon," *J. Atmos. Oceanic Technology*, vol. 16, no. 12, pp. 1973-1993, 1999.
- [13] Youyu Lu and Rolf G. Lueck, "Using a Broadband ADCP in a Tidal Channel. Part II: Turbulence," *J. Atmospheric and Oceanic Tech.*, vol. 16, pp. 1568-1579, November 1999.
- [14] Kristen Thyng, "State of NNMREC Modeling," University of Washington NNMREC, Seattle, Presentation 2008.
- [15] Mary Ann Adonizio, Hannah Abend, Susana Crespo, and Dean Corren, "NPS - Stationary ADCP locations - Work under CDRL A009," Verdant Power, New York, Memorandum 2008.
- [16] Roger Bedard, "Survey and Characterization: Tidal In Stream Energy Conversion (TISEC) Devices," in *EPRI North American Tidal In Stream Power Feasibility Demonstration Project.*: EPRI, 2005.
- [17] David R. Wilkinson, "A study of flow acceleration over a coastal headland," Oregon State University, Corvallis, MS Thesis 1979.
- [18] Pijush Kundu and Ira Cohen, *Fluid Mechanics*. San Diego: Academic Press, 2002.
- [19] Erik L. Petersen, Niels G. Mortensen, Lars Landberg, Jørgen Højstrup, and Helmut P. Frank, "Wind Power Meteorology," Risø National Laboratory, Roskilde, Denmark, 1997.
- [20] "Acoustic Doppler Current Profiler Principles of Operation: A Practical Primer.," RDI Instruments, 1996.
- [21] Phillip J Wiles, Tom P Rippeth, John Simpson, and Peter J. Hendricks, "A novel technique for measuring the rate of turbulent dissipation in the marine environment," *Geophysical Research Letters*, vol. 33, no. L21608, November 2006.
- [22] H Sauvageot, *Radar Meteorology*. Norwood, Mass.: Artech House, 1992.
- [23] Simon P. Neilla, Emmer J. Litta, Scott J. Couch, and Alan G. Daviesa, "The impact of tidal stream turbines on large-scale sediment dynamics," *Renewable Energy*, vol. 34, p. 2803-2812, June 2009.
- [24] E.W. Peterson and J.P. Hennessey Jr., "On the use of power laws for estimates of wind power potential," *J. Appl. Meteorology*, vol. 17, pp. 390-394, 1978.
- [25] NOAA National Geophysical Data Center. (2006, May) GEODAS Grid Translator - Design-a-Grid. [Online]. [http://www.ngdc.noaa.gov/mgg/gdas/gd\\_designagrid.html](http://www.ngdc.noaa.gov/mgg/gdas/gd_designagrid.html)
- [26] Robert Stewart, *Introduction to physical oceanography*. Austin, 2008.
- [27] Adrian E. Gill, *Atmosphere-ocean dynamics*. San Diego: Academic Press, 1982.